Systematic Study of the Effect of Lower-Rim Methylation on Small Guest Binding within the Host Cavity of Calix[4]arene

Systematic Study of the Effect of Lower Rim Methylation on Small Guest Binding within the Host Cavity of Calix[4]arene

*Paul Murphy, Scott J. Dalgarno, Martin J. Paterson**

Institute of Chemical Sciences, Heriot Watt University, Edinburgh EH14 4AS, United Kingdom

ABSTRACT: The efficacy of calixarenes for the storage and/or detection of small guest molecules at the upper rim is well known. As part of our continuing efforts to investigate the ability to fine-tune the structure and hence host-guest binding characteristics of calixarenes, we present a systematic investigation of the effect of methylation of the lower rim tetraphenolic pocket of calix[4]arene (C[4]) on the binding at the upper rim for a test-suite of guest molecules consisting of H_2, O_2, N_2, H_2O, CO_2, NH_3, H_2S, N_2O, HCN and SO_2. Results of the effects on the host-guest binding for all permutations of single, double, triple and quadruple methylations are presented. It was found that whilst a tetraphenolic C[4] host does not discriminate between many of the guest molecules in terms of binding energies, progressively methylated lower-rim C[4] hosts introduce differences in guest binding energies within the upper cavity to the extent where it may be possible to competitively bind one guest over another over a wide range of guests. In this regard, this family of methylated C[4] hosts show promise as gas separation devices.

Introduction

Calix[*n*]arenes[1] are macrocyclic oligomeric structures consisting of *n* phenolic rings connected by methylene bridges, forming a "cup-like" molecule, an example of which is *p*-tert-butylcalix[4]arene (TBC[4]) shown in Figure 1. As can be seen, four stable conformations are possible with the cone conformation the most thermodynamically stable.

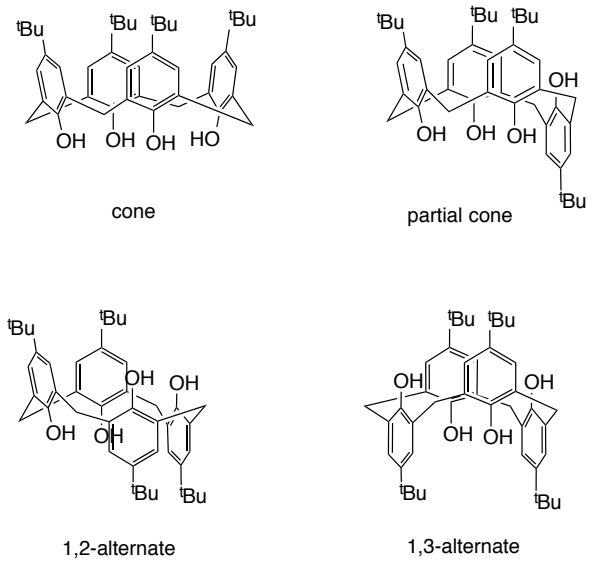

Figure 1. Stable confirmations of TBC[4]

First discovered[2] by Zinke *et al*. in 1941, the tetrameric structure of TBC[4] was not confirmed until the 1950s as a result of work[3,4] by Cornforth *et al*. to discover phenolic based molecules with suitable anti-tuberculous properties. Calixarenes subsequently found industrial application in the synthesis of phenol based resins[5,6] although this proved extremely challenging with complicated protection groups required to allow adequate control over the reactions. As a result of these difficulties, calixarenes remained relatively obscure until the discovery of a simple one-

pot synthesis[7] by Gutsche *et al*. This discovery transformed the field allowing calixarenes to gain much prominence in scientific literature. Advances[8,9,10,11,12] included substitution at the methylene bridges, the para position and at the tetraphenolic pocket.

As seen in Figure 1, the cone conformation results in hydrogen bonding at the calixarene lower rim. Deprotonation at the lower rim in the presence of transition metal and/or lanthanide salts was found to permit the formation of polymetallic clusters[13,14,15,16,17,18] displaying a range of properties including magnetism and refrigeration. Two examples of polymetallic clusters are shown in Figure 2 and Figure 3, using calix[4]arene (C[4]). More recent work has expanded polymetallic clusters to include bis-calixarenes,[12,19,20,21] formed by substituting one of the hydrogen atoms at a methylene bridge with a second calixarene.

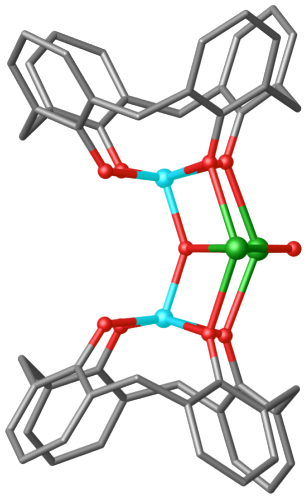

Figure 2. Polymetallic TBC[4] cluster containing Fe(III) and Gd(III).[16]

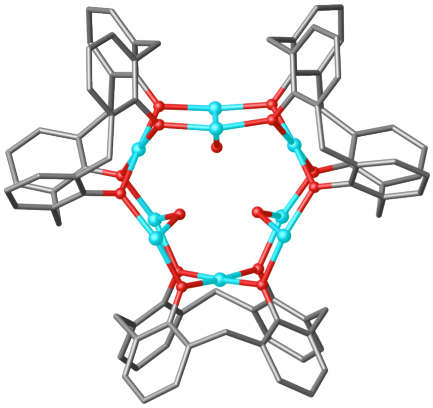

Figure 3. Polymetallic TBC[4] cluster containing Cu(II).[17]

The use of calixarenes to detect and store small guest molecules in the upper rim cavity has a rich and varied history. Early efforts[22] forced the calixarene into the cone conformation using bridging ligands at the upper rim, allowing storage of small organic guest molecules such as alcohols and esters. A major problem with these structures however was fracturing of the substrate. Removing the bridging ligand[23] at the upper rim resolved this issue. With the calixarene then able to interconvert between different conformations outlined in Figure 1, guest molecules were found to engage in a process of Dynamic Transport where the guest would be temporarily trapped within one calixarene entity in the cone conformation before being released when other conformations were adopted over time. It was realized that this allowed guests to diffuse throughout the storage medium with obvious benefits in terms of storage capacity, throughput and subsequent controlled release[24,25,26,27,28] of the gas. Following these advances, calixarenes have found application in areas such as storage of toxic and unstable compounds,[29] gas phase optical detectors[30] and the environmental detection of silver ions,[31] fluoride ions,[32] arsenic,[33] NADH[34] and dopamine.[35]

Recently, our own investigations found that the use of polymetallic clusters had an impact on binding strengths of guests at the upper rim[18,36] and in this work, we aim to continue our investigations into finely tuned control of guest binding within C[4]. We undertake a theoretical study, using DFT, of the effect of progressive methylation of the lower-rim tetraphenolic pocket of C[4] on the binding energies of a range of small guest molecules at the upper rim.

Computational Details

All calculations were performed using Gaussian 09 D.01.[37] Geometry optimisations for all computed structures were initially performed using B3LYP/cc-pVDZ with GD3BJ empirical dispersion,[38,39,40,41] followed by a further single point calculation using B3LYP/cc-pVTZ with GD3BJ empirical dispersion to obtain more accurate energies. Justification for the choice of method was provided in our previous work.[12,18,36] Energy values are internal reaction energies corrected for zero-point energy with no symmetry constraints applied. Geometry optimisation was checked by analysis of the analytical Hessian, which confirmed the nature of the critical points as minima via the absence of imaginary eigenvalues. Basis set superposition error corrections were made to binding energies using the Counterpoise correction methodology within the Gaussian program[42,43] using single point cc-pVTZ calculations at the cc-pVDZ geometry. To calculate binding energies the following is used:

$$E_{bind} = E_{complex} - E_{gas} - E_{C[4]}$$

Here, $E_{complex}$ is the zero-point corrected internal energy of the geometry-optimised, bound calixarene-guest complex which already contains the counterpoise correction as calculated by Gaussian, E_{gas} is the zero-point energy corrected internal energy of the geometry-optimised free gas molecule and $E_{C[4]}$ is the zero-point energy corrected internal energy of the geometry-

optimised free C[4] molecule in the cone conformation. Finally, NBO3.0 calculations were performed at the B3LYP/cc-pVTZ level using GD3BJ empirical dispersion using Gaussian 09 D.01.

Results and Discussion

The current study consists of the following C[4] host molecules shown in Figure 4. The test-bed of guest molecules for binding to the C[4] upper rim are: H_2, N_2, O_2, CO_2, H_2O, NH_3, HCN (both linkage isomers), SO_2 (both linkage isomers), H_2S and N_2O (both linkage isomers). Overall results are shown in Table 1 and Figure 5. The relative percentage changes in binding energy of the guests for each methylated C[4] compared to the original tetraphenolic C[4] is shown in Table 2.

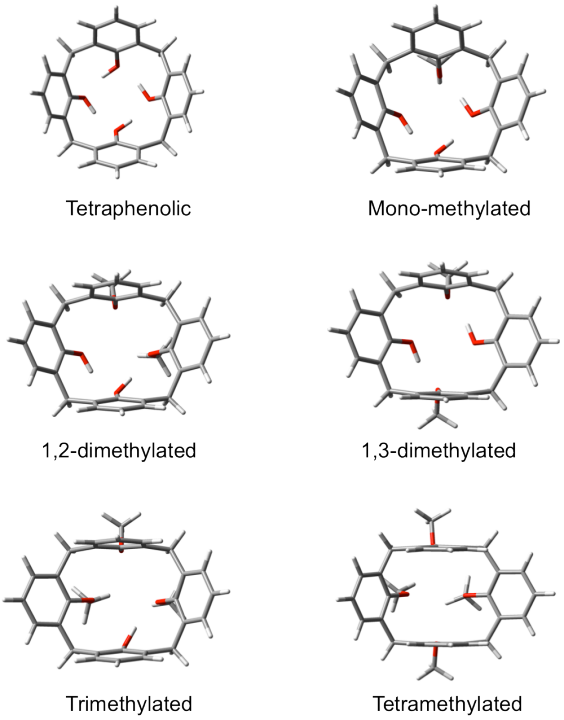

Figure 4. Progressively methylated calix[4]arenes. Shown looking into annulus from upper rim.

Table 1. Binding energies (kcalmol^{-1}) for guest gas molecules at the upper rim of a variety of lower-rim methylated calixarenes. B3LYP/cc-pVTZ and GD3BJ empirical dispersion are used. All results BSSE corrected. Guests with a letter in parentheses bind to C[4] with this atom pointing down into the cavity.

Bound Gas	**tetraphenolic**	**monomethylated**	**1,2-dimethylated**	**1,3-dimethylated**	**trimethylated**	**tetramethylated**
H_2	-1.72	-1.73	-1.43	-0.95	-2.86	0.03
O_2	-3.43	-3.41	-3.27	-2.90	-4.25	-0.43
N_2	-5.24	-5.18	-4.51	-4.31	-4.95	-1.22
H_2O	-4.62	-5.32	-4.96	-3.81	-6.08	-4.65
N_2O (O)	-5.97	-6.35	-6.53	-6.28	-7.66	-3.90
CO_2	-6.75	-6.94	-7.09	-6.78	-8.09	-4.35
N_2O (N)	-6.73	-6.78	-6.91	-6.54	-6.23	-4.16
NH_3	-7.21	-6.49	-5.36	-4.53	-4.97	-1.68
HCN (C)	-7.71	-8.93	-9.03	-8.74	-11.08	-8.03
HCN (N)	-7.43	-8.92	-9.02	-8.74	-11.08	-8.03
H_2S	-8.69	-9.39	-8.22	-7.43	-7.01	-3.29
SO_2 (S)	-10.66	-11.39	-12.22	-11.13	-13.17	-9.71
SO_2 (O)	-11.19	-11.81	-12.17	-11.21	-13.12	-9.71

Table 2. Relative percentage change in binding energies ($kcalmol^{-1}$) for guest molecules at the upper rim when the methylation changes at the lower rim. B3LYP/cc-pVTZ and GD3BJ empirical dispersion are used. All results BSSE corrected. A negative value means that the strength of the binding has reduced. Guests with a letter in parentheses bind to C[4] with this atom pointing down into the cavity.

Bound Gas	tetraphenolic	monomethylated	1,2-dimethylated	1,3-dimethylated	trimethylated	tetramethylated
H_2	0.00	0.58	-16.86	-44.770	+66.28	-101.74
O_2	0.00	-0.58	-4.66	-15.45	+23.91	-87.46
N_2	0.00	-1.15	-13.93	-17.75	-5.53	-76.22
H_2O	0.00	+15.15	+7.36	-17.53	+31.60	+0.65
N_2O (O)	0.00	+6.37	+9.38	+5.19	+28.31	-34.67
CO_2	0.00	+2.81	+5.04	+0.44	+19.85	-35.56
N_2O (N)	0.00	+0.74	+2.67	-2.82	-7.43	-38.19
NH_3	0.00	-9.99	-25.66	-37.17	-31.07	-76.70
HCN (C)	0.00	+15.82	+17.12	+13.36	+43.71	+4.15
HCN (N)	0.00	+20.05	+21.40	+17.63	+49.13	+8.08
H_2S	0.00	+8.06	-5.41	-14.50	-19.33	-62.14
SO_2 (S)	0.00	+6.85	+14.63	+4.41	+23.55	-8.91
SO_2 (O)	0.00	+5.54	+8.76	+0.18	+17.25	-13.23

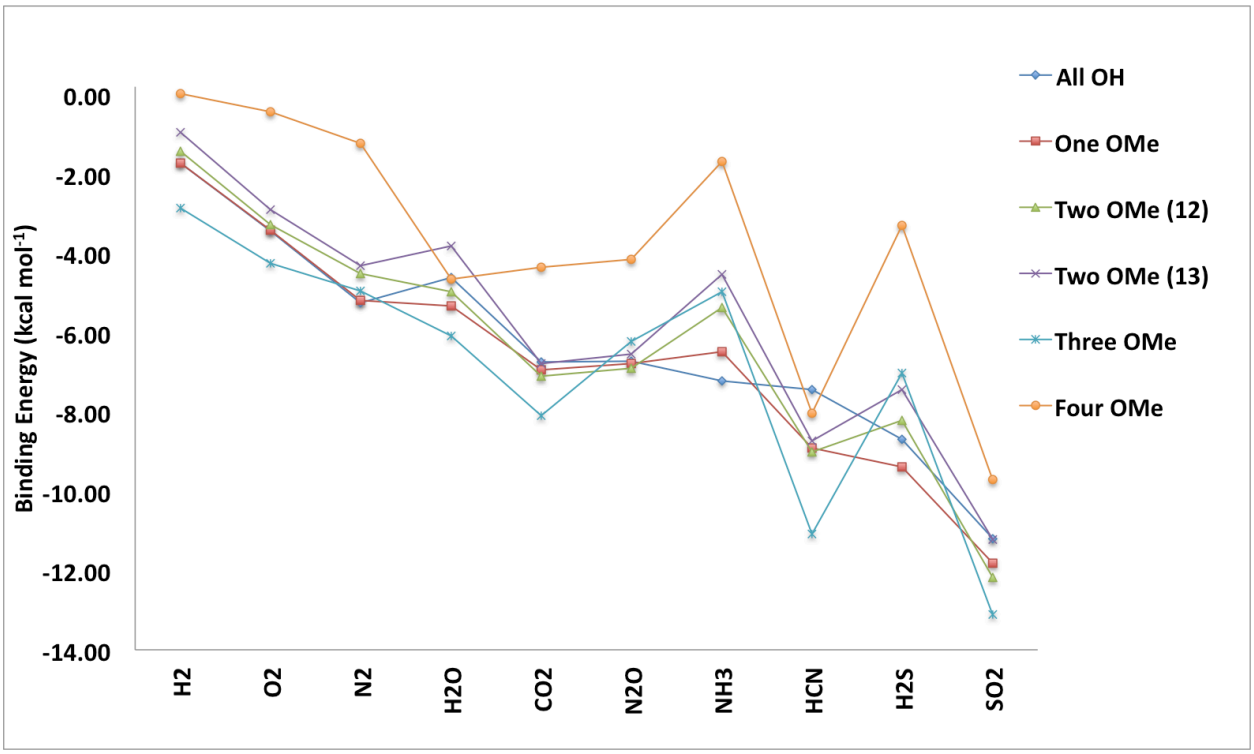

Figure 5. Binding energies of gas molecule guests to upper rim of various calixarenes with a range of methylated positions at the lower rim.

As can be seen from Table 1, results indicate that the binding energies of the two binding forms of HCN are indistinguishable from each other and by choice we consider only HCN with the N atom pointing into the cavity in further discussion. A similar story is seen with both N_2O, where we only consider the binding arrangement with the N atom pointing into the cavity, and also with SO_2, where we only consider the binding arrangement with the O atom pointing into the cavity.

Starting from tetraphenolic C[4], where the nature of binding has been discussed in our previous work,[36] we now present the effect of methylation of the lower rim on the binding of the guest molecules.

Mono-methylated C[4]

Compared to tetraphenolic C[4], the general trend of binding energies here shows few significant changes. The sulfonated compounds and water experience a stronger binding of around 0.7 $kcalmol^{-1}$. The largest effect occurs with HCN, which experiences around 1.5 $kcalmol^{-1}$ strengthening. NH_3 on the other hand experiences a weakening of its binding by around 0.7 $kcalmol^{-1}$. For SO_2, the effect of single methylation is shown in Figure 6. Here it can be seen that the opposing phenyl groups in the horizontal plane have closed by around 0.3 Å at the upper rim. Although there is one less OH moiety for SO_2 with mono-methylated C[4], to bind to, the closing of the upper rim seems to have the greater effect. There are no significant geometric alterations elsewhere in the C[4] or in the positioning of the guest within the host. A similar "pinching" effect is seen with H_2S. For H_2O, and HCN, the pinching happens to a lesser degree but the effect is seen both horizontal and vertical directions. Although this "pinching" increases binding strength, this effect is partly countered by the reduction in hydrogen bonding available. Finally, NH_3 is considered. This is affected by the same pinching above but because the lone pair is more available than that of water, the most significant change will be the loss of one of the OH moieties at the lower rim, the net effect of which is a weakening of the binding of this guest.

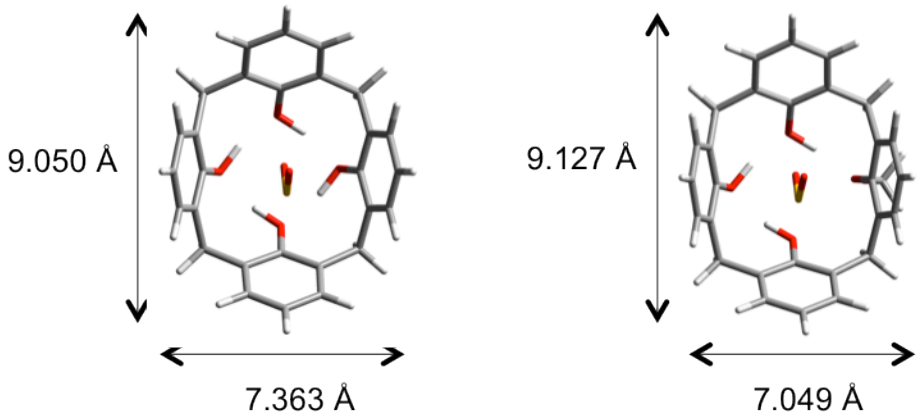

Figure 6. Effect of mono-methylation at lower rim of C[4] on binding of SO_2. On the left is tetraphenolic C[4] and on the right is mono-methylated C[4]. Here, the "pinching" effect between opposite phenyl rings at the upper rim is seen.

Di-methylated C[4]

There appears to be a small difference in binding strengths between 1,2- and 1,3-dimethylated C[4] with 1,3-dimethylated C[4] providing weaker binding by between around 0.2 kcalmol^{-1} and 1.2 kcalmol^{-1}, the latter value that of H_2O binding. We shall consider the 1,3- variant as this has the greatest effect compared to tetraphenolic C[4]. The guests experiencing the greatest effect are seen to be NH_3, which experiences a reduction in binding energy of around 2.7 kcalmol^{-1}, H_2S which experiences a reduction in binding strength of 1.3 kcalmol^{-1} and HCN which experiences an increase in binding strength by around 1.3 kcalmol^{-1}. For NH_3 and H_2S, there is a further reduction in OH moieties at the lower rim in the di-methylated C[4] with only two present which causes further weakening of the binding of the guest. The effect on HCN of 1,3-dimethylation is dramatically shown in Figure 7. Here the entire guest molecule is seen to rotate to bind with the H atom now pointing downwards into the cavity as clearly shown by the side view at the bottom of the figure. NBO analysis shows that the greatest stability is achieved when a lone pair on the

O atoms of each of the remaining OH moieties of the lower rim binds to the C-H σ–bond of the guest.

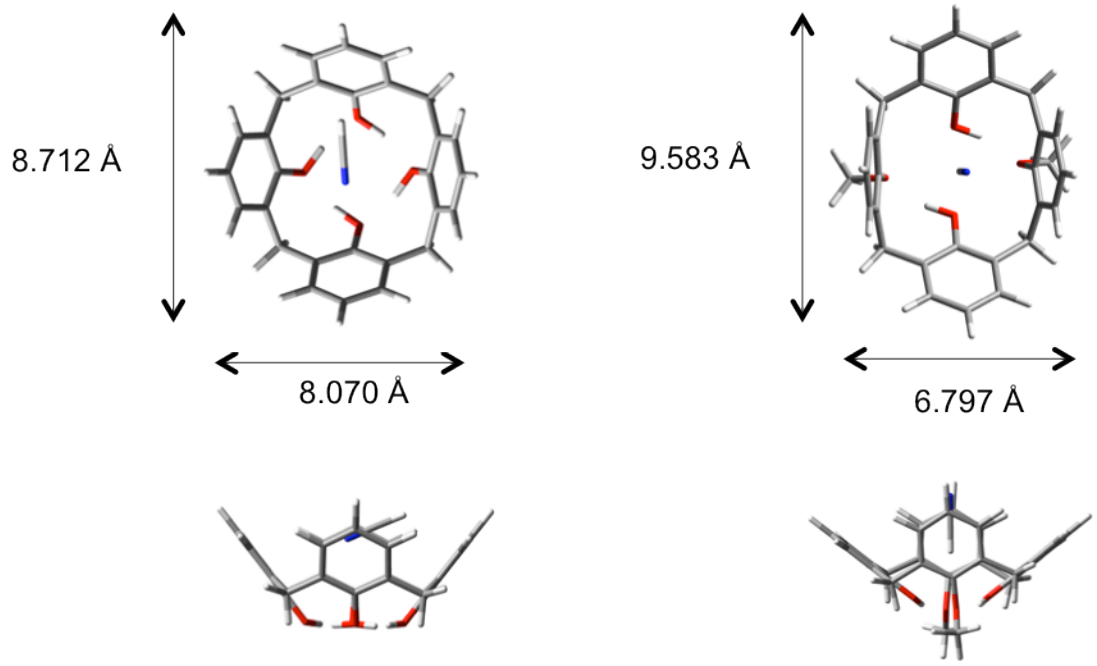

Figure 7. Effect of 1,3-dimethylation at lower rim of C[4] on binding of HCN. On the left is tetraphenolic C[4] and on the right is 1,3-dimethylated C[4]. Here, a dramatic "pinching" effect between opposite phenyl rings at the upper rim is seen. The guest has also flipped upside down with the H atom now pointing down into the cavity. The side views clearly show the inversion of the guest in the upper cavity.

Tri-methylated C[4]

Upon tri-methylation, the impact upon the guest molecules is more severe than for either mono- or di-methylated cases. Guests such as O_2, H_2, CO_2, H_2O and SO_2 now experience a strengthening of binding of around 1 to 2 kcalmol^{-1}. H_2S on the other hand experiences reduced binding strength of 1.68 kcalmol^{-1}. NH_3 and HCN experience the strongest impact however with

reduced binding strengthens of 2.24 kcalmol^{-1} and an increase in binding strength of 3.65 kcalmol^{-1} respectively. The situation with HCN is very similar to that for dimethylated C[4]. A complete inversion of the guest with the upper cavity occurs. This is shown in Figure 8. NBO analysis shows that this time however, the greatest stability is achieved when a lone pair on one of the methylated O atoms of the lower rim binds to the C-H σ–bond.

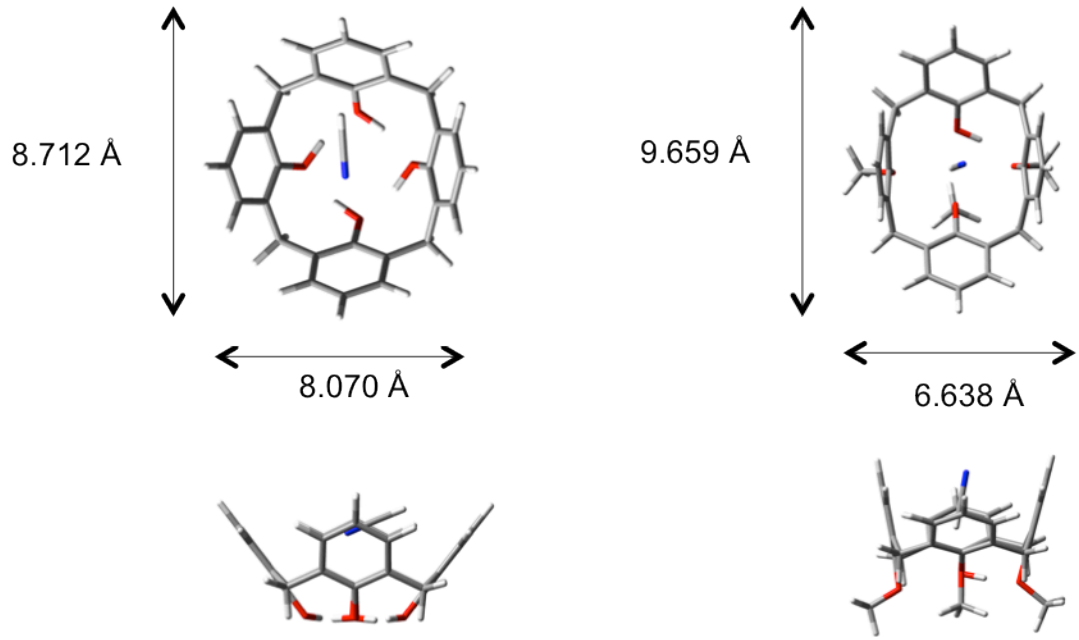

Figure 8. Effect of trimethylation at lower rim of C[4] on binding of HCN. On the left is tetraphenolic C[4] and on the right is trimethylated C[4]. Here, a dramatic "pinching" effect between opposite phenyl rings at the upper rim is seen. The guest has also flipped upside down with the H atom now pointing down into the cavity. The side views clearly show the inversion of the guest in the upper cavity.

For NH_3, the π–bonding which stabilised the guest binding within tetraphenolic C[4] is disrupted in trimethylated C[4] and the guest molecule is seen to rotate in the upper cavity. This represents a weakening of the guest binding with NBO analysis indicating that the dominant host-guest

interaction is now between the lone pair on one of the methylated O atom on the calixarene and the N-H σ–bond of the guest. This is shown in Figure 9.

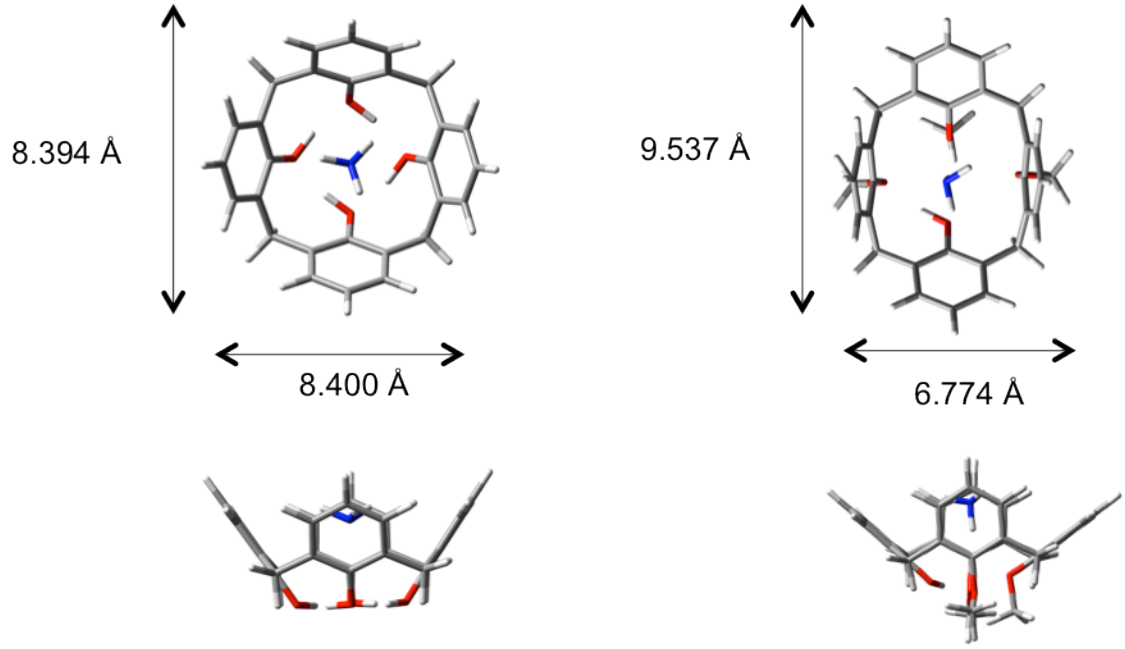

Figure 9. Effect of trimethylation at lower rim of C[4] on binding of NH_3. On the left is tetraphenolic C[4] and on the right is trimethylated C[4]. Here, a dramatic "pinching" effect between opposite phenyl rings at the upper rim is seen. The guest has also rotated considerably within the cavity.

Tetra-methylated C[4]

For tetramethylated C[4], substantial changes to host-guest binding strengths are observed. With the exception of HCN and H_2O, all other guests experience a weakening of binding to the host of between 1.5 kcalmol^{-1} (for SO_2) and 5.53 kcalmol^{-1} (for NH_3). In particular, H_2 is now predicted to be unbound, with O_2 and N_2 now very weakly-bound. For all species except NH_3, there is no

change in the nature of the binding of the guest to the host – simply a reduction in strength of those bindings as a result of the change in geometry at the upper rim. NH_3 binding changes from predominantly a N atom lone pair donation into the aromatic rings of the upper rim for tetraphenolic C[4], to donation from the aromatic ring of the upper rim into the N-H σ–bond in tetramethylated C[4]. This results in weaker binding of the guest within the host cavity as is shown in Figure 10.

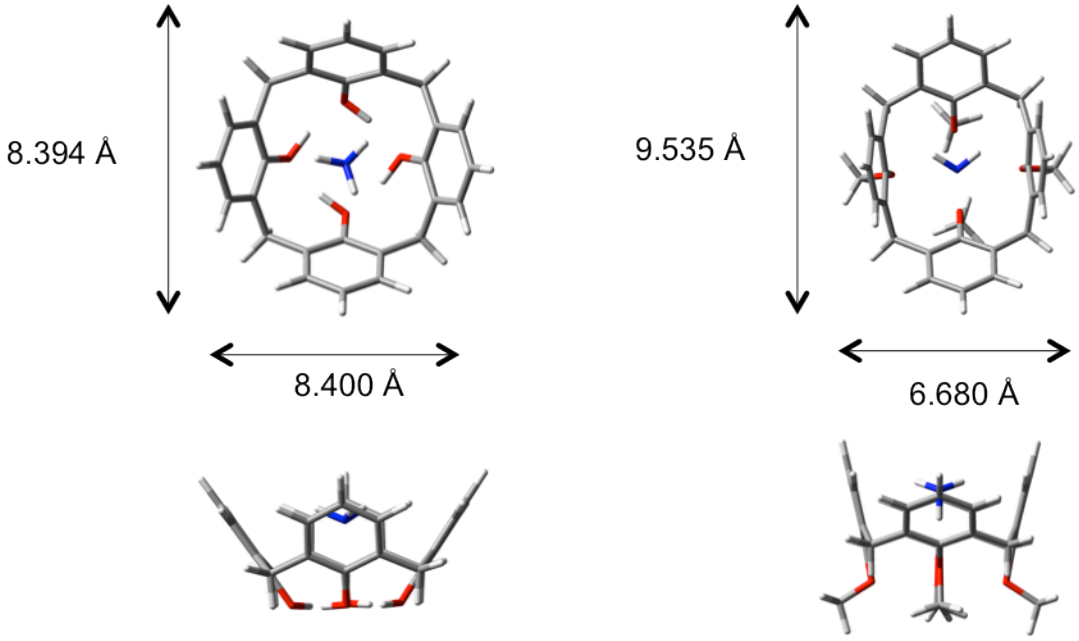

Figure 10. Effect of tetramethylation at lower rim of C[4] on binding of NH_3. On the left is tetraphenolic C[4] and on the right is tetramethylated C[4]. Here, a dramatic "pinching" effect between opposite phenyl rings at the upper rim is seen. The guest has also rotated considerably within the cavity.

We now move from the changes in binding to a discussion of the consequences for host-guest binding using these calixarene species. Figure 4 has been modified to separate out the individual

methylated C[4] species in order to allow overall trends to be identified as shown in Figure 11 to Figure 16.

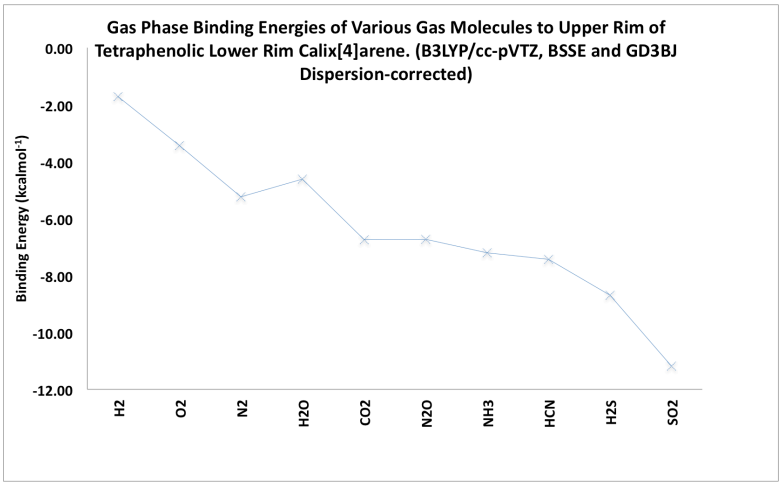

Figure 11. Tetraphenolic C[4] guest binding. Here it can be seen that there is little discrimination between guests such as CO_2, N_2O, NH_3 and HCN. All have relatively similar binding strengths to the C[4] upper rim.

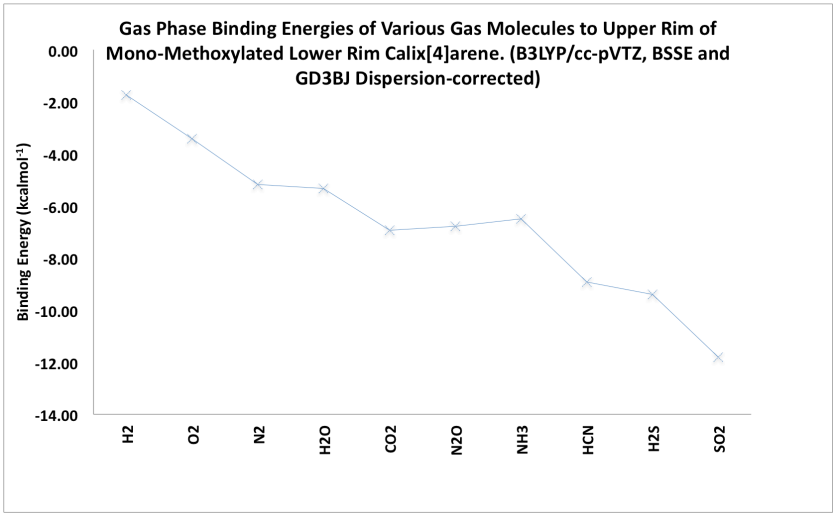

Figure 12. Mono-methylated C[4] guest binding. Here it can be seen that some discrimination for NH_3 and HCN is beginning to show.

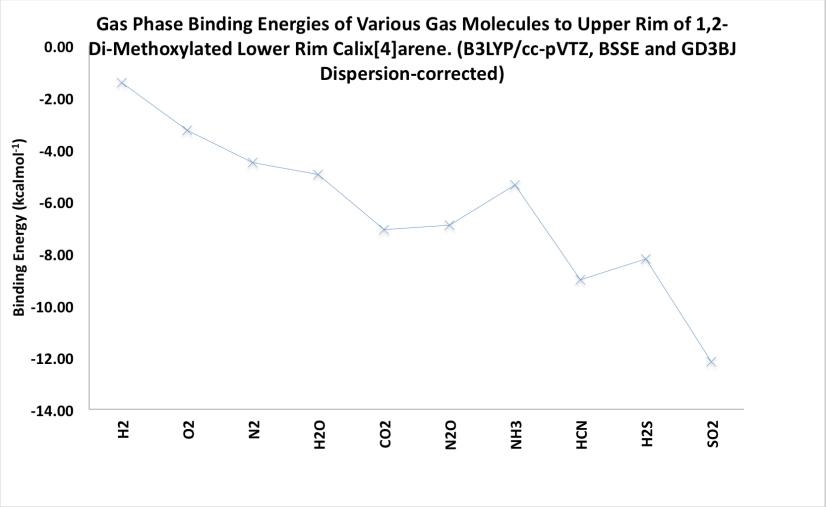

Figure 13. 1,2-dimethylated C[4] guest binding. The discrimination towards NH_3 and HCN is becoming more pronounced. Binding energies for CO_2 and N_2O are now starting to drift apart.

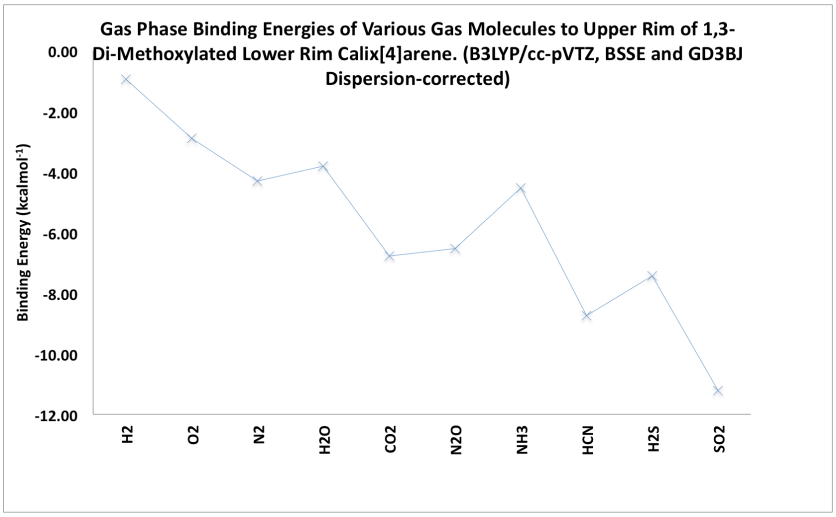

Figure 14. 1,3-dimethylated C[4] guest binding. Further splitting of binding energies is seen here.

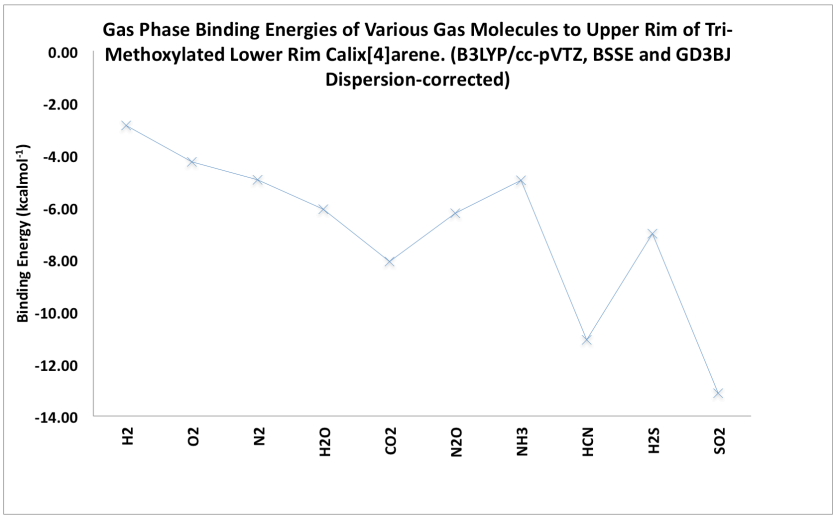

Figure 15. Trimethylated C[4] guest binding. Most guests can now be individually discriminated.

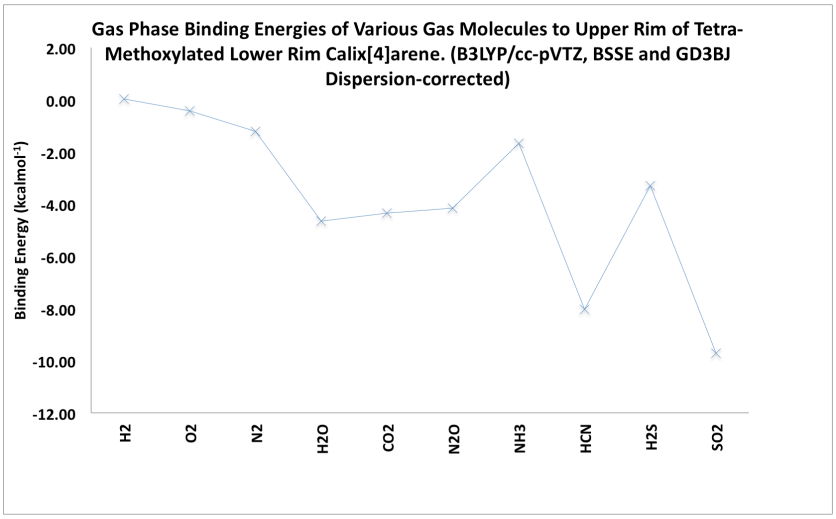

Figure 16. Tetramethylated C[4] guest binding. N_2O, NH_3 and HCN are now well separated in binding energies suggesting a mixture of these gases could be separated by tetramethylated C[4].

The key characteristic of tetraphenolic C[4] is that many guests share a very similar binding strength at the upper cavity. For example, CO_2, N_2O, NH_3 and HCN binding strengths are separated by less than 1 kcalmol^{-1}. This would cause problems if these gases were to be separated

using tetraphenolic C[4]. By using trimethylated C[4] however, the situation is dramatically different as shown in Table 1 and Figure 15. Here, CO_2 and N_2O, for example have a binding difference of almost 1.9 kcalmol^{-1} for trimethylated C[4] instead of just 0.02 kcalmol^{-1} for tetraphenolic C[4], whilst NH_3 and NH_3 are separated by over 6 kcalmol^{-1} for trimethylated C[4] compared to just 0.22 kcalmol^{-1} for tetraphenolic C[4]. As a general rule, the trend is for greater separation of the binding energies of guest molecules as methylation of the lower rim is increased, leading to the prospect of increasingly fine control over which guests preferentially bind in a mixture of gases. Our work suggests that progressively methylating the lower rim of C[4] would allow separation or selective uptake of gases which would otherwise show no preferential affinity for tetraphenolic C[4].

Summary and Conclusions

Our work has shown that progressively methylating the lower rim of tetraphenolic C[4] shows promise for gas separation applications. Our calculations predict that whilst tetraphenolic C[4] shows no particular preference for many of the guests in our study, this is not the case for trimethylated C[4] and tetramethylated C[4]. Our inclusion of monomethated C[4] and dimethylated C[4] clearly demonstrates the progressive nature of increasing methylation on discrimination of these guest molecules, indicating potential for a measure of fine control and tuning. It is known from the work of Barbour *et al*., [27] that performing the type of experimental study necessary to progress our studies will require significant amounts of amounts of prior structural work, which is beyond the scope of this initial theoretical study. We hope that our initial theoretical studies will underpin future experimental work in this area.

Corresponding Author

* Martin J. Paterson: phone, +44 (0)131 451 8035; email, M.J.Paterson@hw.ac.uk

Acknowledgements

MJPl would like to thank the European Research Council (ERC) for funding under the European Union's Seventh Framework Programme (FP7/2007-2013)/ERC Grant No. 258990; and the EPSRC for funding through the platform grant EP/P001459/1; PM would like to thank the EPSRC for DTP Studentship funding.

References

1. Steed, J.; Atwood J.L. *Supramolecular Chemistry*, John Wiley & Sons: Hoboken, NJ, **2009**

2. Zinke, A.; Ziegler, E. Zur Kenntnis des Hartungsprozesses von Phenol Formaldehyd-Harzen, X. Mitteilung. *Chem. Ber.*, **1944**, *77*, 264-272.

3. Cornforth, J.; D'Arcy, P.; Nicholls, G.; Rees, R.; Stock, J. Antituberculous Effects of Certain Surface Active Polyoxyethylene Ethers. *Brit. J. Pharm.* **1955**, *10*, 73-86.

4. Cornforth, J.; Morgan, E.; Potts, K.; Rees, R. Preparation of Antituberculous Polyoxyethylene Ethers of Homogenous Structure. *Tetrahedron*, **1973**, *29*, 1659-1667.

5. Hayes, B.; Hunter, R. Rational Synthesis of Cyclic Tetranuclear Para-Cresol Novolak. *Chem. Ind. (Lond.)*, **1956**, 193-194.

6. Hayes, B.; Hunter, R. Phenol Formaldehyde and Allied Resins VI: Rational Synthesis of a Cyclic Tetranuclear P-Cresol Novolak. *J. Appl. Chem.*, **1958**, *8*, 743-748.

7. Gutsche, D.; Iqbal, M.; Stewart, D. Calixarenes. 18. Synthesis Procedures For *p*-tert-Butylcalix[4]arene. *J. Org. Chem.*, **1986**, *51*, 742-745.

8. Ikeda, A.; Shinkai, S. Novel Cavity Design Using Calix[n]arene Skeletons: Toward Molecular Recognition and Metal Binding. *Chem. Rev.*, **1997**, *97*, 1713-1734.

9. Katz, J. L.; Feldman, M. B.; Conry, R. R. Synthesis of Functionalised Oxacalix[4]arenes. *Organic Letters*, **2005**, *7*, 91-94.

10. Maes, W.; Van Rossom, W.; Van Hecke, K.; Van, Meervelt, L. Synthesis of Functionalised Thia- and Oxacalix[2]arene[2]pyrimidines. *Organic Letters*, **2006**, *8*, 4161-4164.

11. Carroll, L. T.; Hill, P. A.; Ngo, C. Q.; Klatt, K. P.; Fantini, J. L. Synthesis and Reactions of a 2-Chlorocalix[4]arene and a 2,2'-Coupled Dicalixarene. *Tetrahedron*, **2013**, *69*, 5002-5007.

12. Murphy, P; Dalgarno, S. J.; Paterson, M. J. Elucidating the Ring Inversion Mechanism(s) for Biscalixarenes, *J. Phys. Chem. A*, **2014**, *118*, 7986-8001.

13. Castellano, B.; Solari, E.; Floriani, C.; Scopelliti, R. Reactivity Of A Vanadium(III) Center over an Oxo Surface Modeled by Calix[4]arene. *Inorg. Chem.*, **1999**, *38*, 3406-3413.

14. Karotsis, G.; Teat, S. J.; Wernsdorfer, W.; Piligkos, S.; Dalgarno, S. J.; Brechin, E. K. Calix[4]arene-Based Single Molecule Magnets. *Angew. Chem. Int. Ed.*, **2009**, *48*, 8285-8288.

15. Taylor, S. M.; McIntosh, R. D.; Pilikgos, S.; Dalgarno, S. J.; Brechin, E. K. Calixarene-supported Clusters: Employment of Complementary Cluster Ligands for the Construction of a Ferromagnetic [Mn_5] Cage. *Chem. Commun.*, **2012**, *48*, 11190-11192.

16. Sanz, S.; Ferreira, K.; McIntosh, R. D.; Dalgarno, S. J.; Brechin, E. K. Calix[4]arene-Supported $Fe^{III}_2Ln^{III}_2$ Clusters. *Chem. Commun.*, **2011**, *47*, 9042-9044.

17. Karotsis, G.; Kennedy, S.; Dalgarno, S. J.; Brechin, E. K. Calixarene Supported Enneanuclear Cu(II) Clusters. *Chem. Commun*, **2010**, *46*, 3884-3886.

18. Murphy, P.; McKinlay, R.; Dalgarno, S. J.; Paterson, M. J. Towards Understanding of the Lower-Rim Binding Preferences of Calix[4]arene. *J. Phys. Chem. A*, **2015**, *119*, 5804-5915.

19. Coletta, M.; McLellan, R.; Cols, J-M.; Gagnon, K.; Teat, S.; Dalgarno S. J. Investigations into Cluster Formation with Alkyl Tethered Bis-calix[4]arenes. *Supra. Chem.*, **2016**, *28*, 5-6, 557-566.

20. Coletta, M.; McLellan, R.; Waddington, A.; Sanz, S.; Gagnon, K.; Teat, S.; Brechin, E. K.; Dalgarno, S. J. Core Expansion of Bis-calix[4]arene supported Clusters. *Chem. Comm.*, **2016**, *52*, 14246-14249.

21. Coletta, M.; McLellan, R.; Murphy, P.; Leube, B. T.; Sanz, S.; Clowes, R.; Gagnon, K. J.; Teat, S. J.; Cooper, A. I.; Paterson, M. J., et al. Bis-calixa[4]arenes: From Ligand Design to the Directed Assembly of a Metal-Organic Trigonal Antiprism. *Chem. Eur. J.*, **2016**, *22*, 8791-8795.

22. Arduini, A.; Cantoni, M.; Graviani, E.; Pochini, A.; Secchi, A.; Sicuri, A.; Ungari, R.; Vincenti, M. Gas Phase Complexation of Neutral Molecules by Upper Rim Bridged Calix[4]arenes. *Tetrahedron*, **1995**, *51*, 2, 599-606.

23. Atwood, J. L.; Barbour, L. J.; Jerga, A.; Schottel, B. L. Guest Transport in a Nonporous Organic Solid via Dynamic van der Waals Cooperativity. *Science*, **2002**, *298*, 1000-1002.

24. Adams, J. E.; Cox, J. R.; Christiano, A. J.; Deakyne, C. A. Molecular Dynamics of Host-Guest Complexes of Small Gas Molecules with Calix[4]arenes. *J. Phys. Chem. A*, **2008**, *112*, 6829-6839.

25. Enright, G. D.; Udachin, K. A.; Moudrakovski, I. L; Ripmeester, J. A. Thermal Programmable Gas Storage and Release in Single Crystals of an Organic van der Waals Host. *J. Am. Chem. Soc.*, **2003**, *125*, 9896-9897.

26. Atwood, J. L.; Barbour, L. J.; Thallapally, P. K.; Wirsig T.B. A Crystalline Organic Substrate Absorbs Methane under STP. *Chem. Commun.*, **2005**, 51-53.

27. Thallapally, P. K.; Wirsig, T. B.; Barbour, L. J.; Atwood, J. L. Crystal Engineering of Nonporous Organic Solids for Methane Sorption. *Chem. Commun.*, **2005**, 4420-4422.

28. Thallapally, P. K.; Dobrzanska, L.; Gingrich, T. R.; Wirsig, T. B.; Barbour, L. J.; Atwood, J. L. Acetylene Absorption and Binding in a Nonporous Crystal Lattice. *Angew. Chem. Int. Ed.*, **2006**, *45*, 6506-6509.

29. Zyryanov, G. V.; Kang, Y.; Rudkevich, D. M. Sensing and Fixation of NO_2/N_2O_4 by Calix[4]arenes. *J. Am. Chem. Soc.*, **2003**, *125*, 2997-3007.

30. Liu, C. J.; Lin, J. T.; Wang, S. H.; Jiang, J. C.; Lin, L. G. Chromogenic Calixarene Sensors for Amine Detection. *Sens. and Actuators B*, **2005**, *108*, 521-527.

31. Lofti, B.; Tarlani, A.; Akbari-Moghaddam, P.; Mirza-Aghayan, M.; Peyghan, A.; Muzart, J.; Zadmard, R. Multivalent calix[4]arene-based Flourescent Sensor for Detecting Silver Ions in Aqueous Media and Physiological Environment. *Biosens. Bioelec.*, **2017**, *90*, 290-297.

32. Nemati, M.; Hosseinzadeh, R.; Zadmard, R.; Mohadjerani, M. Highly Selective Colormetric and Fluorescent Chemosensor for Fluoride Based on Fluorenone Armed Calix[4]arene. *Sens. Act. B – Chem.* **2017**, *241*, 690-697.

33. de Namor, A.; Hakawati, N. A.; Hamdan, W. A.; Soualhi, R.; Korfali, S.; Valiente, L. Calix[4]pyrole for the Removal of Arsenic(III) and Arsenic(V) from Water. *J. Hazard. Mater.*, **2017**, *326*, 61-68.

34. Zadmard, R.; Akbari-Moghaddam, P.; Darvishi, S.; Mirza-Aghayan, M. A Highly Selective Fluorescent Chemosensor for NADH Based on Calix[4]arene Dimer. *Tetrahedron*, **2017**, *73*, 5-6, 604-607.

35. Zou, F.; Wu, B.; Wang, A.; Chen, Y.; Koh, K.; Wang, K.; Cheng, H. Signal Amplification and Dual Recognition Strategy for Small Molecule Detection by Surface Plasmon Resonance Based on Calix[4]arene Crown Ether Modified Gold Nanoparticles.

36. Murphy, P.; Dalgarno, S. J.; Paterson, M. J. Transition Metal Complexes of Calix[4]arene: Theoretical Investigations into Small Guest Binding within the Host Cavity. *J. Phys. Chem. A*, **2016**, *120*, 824-839.

37. Frisch, M. J.; Trucks, G. W.; Schlegel, H. B.; Scuseria, G. E.; Robb, M. A.; Cheeseman J. R.; Scalmani, G.; Barone, V.; Mennucci, B.; Petersson, G. A., et al. Gaussian 09, Revision D.01; Gaussian Inc.: Wallingford, CT, **2013**.

38. Becke, A. D. Density Functional Thermochemistry III. The Role of Exact Exchange. *J. Chem. Phys.*, **1993**, *98*, 5648-5652.

39. Lee, C.; Yang, W.; Parr, R. G. Development of the Colle-Salvetti Correlation-Energy Formula into a Functional of the Electron Density. *Phys. Rev. B*, **1988**, *37*, 785-789.

40. Grimme, S. Semiempirical GGA-Type Density Functional Constructed with a Long Range Dispersion Correction. *J. Comput. Chem.*, **2006**, *27*, 1787-1799.

41. Grimme, S.; Ehrlich, S.; Goerigk, L. Effect of Damping Function in Dispersion Corrected Density Functional Theory. *J. Comput. Chem*, **2011**, *32*, 1456-1465.

42. Boys, S. F.; Bernardi, F. Calculation of Small Molecular Interactions by Differences of Separate Total Energies – Some Procedures with Reduced Terms. *Mol. Phys.*, **1970**, *19*, 553-566.

43. Simon, S.; Duran, M.; Dannanberg, J. J. How does Basis Set Superposition Error Change the Potential Surfaces for Hydrogen Bonded Dimers. *J. Chem. Phys.*, **1996**, *105*, 11024-11031.

TOC Graphic